HHS Public Access

Author manuscript

J Immunol. Author manuscript; available in PMC 2015 June 18.

Published in final edited form as:

J Immunol. 2014 April 1; 192(7): 3280–3288. doi:10.4049/jimmunol.1301751.

Antigen-Conjugated Human IgE Induces Antigen-Specific T Cell Tolerance in a Humanized Mouse Model

Günther Baravalle[*], **Alexandra M. Greer**[*], **Taylor N. LaFlam**[†], and **Jeoung-Sook Shin**[*]

[*]Department of Microbiology and Immunology, Sandler Asthma Basic Research Center, University of California San Francisco, San Francisco, CA 94143

[†]Diabetes Center, University of California San Francisco, San Francisco, CA 94143

Abstract

Dendritic cells (DCs) play an important role in immune homeostasis through their ability to present Ags at steady state and mediate T cell tolerance. This characteristic renders DCs an attractive therapeutic target for the induction of tolerance against auto-antigens or allergens. Accordingly, Ag-conjugated DC–specific Abs have been proposed to be an excellent vehicle to deliver Ags to DCs for presentation and tolerance induction. However, this approach requires laborious reagent generation procedures and entails unpredictable side effects resulting from Ab-induced crosslinking of DC surface molecules. In this study, we examined whether IgE, a high-affinity, non–cross-linking natural ligand of FcεRI, could be used to target Ags to DCs and to induce Ag-specific T cell tolerance. We found that Ag-conjugated human IgE Fc domain (Fcε) effectively delivered Ags to DCs and enhanced Ag presentation by 1000- to 2500-fold in human FcεRIα-transgenic mice. Importantly, this presentation resulted in a systemic deletion of Ag-specific T cells and prevented these mice from developing delayed-type hypersensitivity, which is critically dependent on Ag-specific T cell immunity. Thus, targeting FcεRI on DCs via Ag-Fcε fusion protein may serve an alternative method to induce Ag-specific T cell tolerance in humans.

Dendritic cells (DCs) play an important role in immune tolerance (1). Mice lacking DCs spontaneously develop fatal autoimmunity (2), supporting the significant contribution of DCs to the development or maintenance of tolerance. The tolerogenic role of DCs is dependent on steady state self-antigen presentation. At rest, DCs continuously endocytose and present self-antigens (3–5). This presentation results in the unresponsiveness or deletion of self-reactive T cells (3, 6). It also mediates the development of regulatory T cells, a unique T cell subset equipped with potent immune-suppressive functions (7, 8).

Targeting Ags to resting DCs using a DC-specific Ab has been suggested as a potential therapeutic strategy for the induction of tolerance against auto-antigens (9, 10). Injection of

Address correspondence and reprint requests to Dr. Jeoung-Sook Shin, 513 Parnassus Avenue, Box 0414, San Francisco, CA 94143. jeoung-sook.shin@ucsf.edu.

The online version of this article contains supplemental material.

Disclosures

The authors have no financial conflicts of interest.

nonobese diabetic (NOD) mice with a β-cell Ag-fused DEC-205 mAb has been shown to prevent diabetes (11, 12). Injection with myelin oligodendrocyte glycoprotein Ag fused with DEC205 or Langerin mAbs has been shown to suppress experimental autoimmune encephalomyelitis in mice (13, 14). However, it is not known whether these Abs would target DCs in humans as efficiently as in mice, because the protein expression pattern differs significantly between species. Indeed, human DEC-205 is expressed on more leukocyte populations than mouse DEC-205, including B cells, T cells, monocytes, macrophages, and NK cells (15). In addition, it is hard to predict the adverse effects elicited by Ab binding. Because Abs are bivalent, their binding to cells can cross-link cell surface molecules. Surface molecule cross-linking often triggers stimulatory signaling in cells, the outcome of which varies depending on cell type (16–19). Importantly, clinical development of human Abs is challenging, and it requires laborious manufacturing procedures, including the initial generation of mAbs in vivo, followed by extensive modifications of the Abs in vitro (20). Thus, there is a need for an alternative method to target DCs and for an animal model to better gauge its targeting efficacy in humans.

Targeting the high-affinity IgE receptor FcεRI with Ag-conjugated IgE could be a promising alternative method. Whereas FcεRI is expressed only by mast cells and basophils in steady state mice, it is additionally expressed by DCs and monocytes in humans (21). The FcεRIα-chain, a member of the Ig superfamily, binds IgE Fc domain at a 1:1 ratio of receptor to IgE with unusually high affinity (K_d = ~10^{-10} M) (22). When IgE/FcεRI complexes are cross-linked by multivalent Ags, a strong inflammatory signal is transmitted to cells, resulting in degranulation of mast cells and basophils and Ag presentation and cytokine production in DCs and monocytes (21). When bound by IgE alone, however, FcεRI does not transmit signaling in general; however, certain IgE clones, namely cytokinergic IgE, appear to induce signaling through IgE Fv domain (23).

In this study, we examined whether the human IgE Fc domain could be used to induce Ag-specific tolerance in vivo by using the previously described hFcεRIα-transgenic (Tg) mice (24), which express human FcεRIα under the control of its own promoter. We demonstrate that Ag-Fcε fusion proteins strongly bind both human DCs and hFcεRIα-Tg mouse DCs, that such Ags are presented to Ag-specific T cells with a 1000–2500 fold greater efficiency than unlinked Ag are, and that this presentation leads to Ag-specific T cell deletion and tolerance.

Materials and Methods

Mice and cell lines

hFcεRIα transgenic mice (24), SMARTA mice (25), $Foxp3^{GFP}$ mice (26), and U937 cells transfected with hFcεRI (27) have been described previously. The human IgE secreting myeloma cell line U266 was purchased from American Type Culture Collection. B6.SJL-*Ptprc*^{a}*Pepc*^{b}/BoyJ, OT-II, and OT-I mice were purchased from Jackson Laboratory. All mice were housed in the University of California San Francisco (UCSF) animal facility, and all experiments and procedures were performed according to protocols approved by the UCSF Institutional Animal Ethics Committee.

Human blood

Healthy human blood was obtained through an ongoing study under the UCSF Institutional Review Board–approved protocol 10-02596 with informed written consent.

Abs

Abs to human CD3 (HIT3a), CD19 (HIB19), CD56 (MEM188), CD14 (HCD14), HLA-DR (L243), BDCA1 (L161), CD123 (6H6), hFcεRIα (CRA-1), IgE (MHE-18), murine CD49b (Dx5), CD11b (M1/70), GR1 (RB6-8C5), Thy1.1 (HIS51), TCRVα2 (B20.1), TCRVβ5 (MR9-4), CD45.1 (A20), CD11c (N418), MHCII (TIB120), and isotype control Ab to hFcεRIα Ab (mouse $IgG2b_k$, eBMG2b) were purchased from Bio-Legend or eBioscience. Anti-CD131 (JORO50) was purchased from BD Biosciences. Anti–BDCA-3 (M80) and mPDCA1 (JF05-1C2.4.1) were purchased from Miltenyi Biotec. Anti-His (Penta) was purchased from Qiagen. HRP-conjugated Abs were purchased from Biosource

Flow cytometry

Human PBMCs were isolated from whole blood via density gradient centrifugation using Ficoll Plaque Plus (GE Healthcare) (28). Murine blood was collected via cardiac puncture and PBMCs were isolated. Cells were labeled with various cell surface Abs and acquired on a FACS LSRII system (BD Biosciences). Only live (propidium iodide–negative [BioLegend]), singlet cells were used for all data analysis. Murine cells were gated as follows: conventional DC (cDC), $CD11c^+MHCII^+$; plasmacytoid DC (PDC), $mPDCA1^+MHCII^+$; basophil, $Dx5^+CD131^+$; monocyte, $CD11b^+Gr1^{med/low}$; B cell, $CD11c^-MHCII^+SSC^{low}FSC^{low}$ or $CD19^+$.

Construction of Ag-Fcε

hIgE cDNA was cloned from the IgE-secreting myeloma cell line U266 (ATCC) using RT-PCR. The Cε2-Cε4 cDNA was amplified using the following primer pair: 5′-GGAATTCTGCTCCAGGGACTTCACC-3′ and 5′-CGATATCTCAGTGGTGATGGTGATGATGAGAACCACCAGAT-TTACCGGGATTTACAGAC-3′, where the reverse primer encodes for the SGGS-linker and the 6xHIS tagged C-terminal end of the Cε4 sequence. This PCR product was cloned in-frame using *Eco*RI/*Eco*RV digestion into a pcDNA3.1 expression vector (Invitrogen), which had a previously inserted IRES-EGFP downstream of the IgE sequence. A V_k signal sequence (METDTLLLWVLLLWVPGSTGD) followed by SGGS-linker sequences and a *Cla*I cloning site were inserted at the N terminus by *Nhe*I/*Eco*RI digestion using the following DNA oligo molecules: 5′-CTAGCTAGCATGGAGACAGACACACTCCTGCTATGGGTACTGCTGCTCTGGGTT CCAGGTTCCACTGGTGACTCTGGTGGTTCTATCGATTCTGGTGGTTCTGAATTCC-3′ and 5′-GGAATTCAGAACCACCAGAATCGATAGAACCACCAGAGTCACCAGTGGAACCT GGAACCCAGAGCAGCAGTACCCATAGCAGGAGTGTGTCTGTCTCCATGCTAGCT AG-3′. The cDNAs for OVA peptide (ISQAVHAAHAEINEAGR, 323–339) and OVA peptide (SIINFEKL, 257–264) were cloned from pCI-neo-cOVA plasmid (Addgene) using RT-PCR. The primer pair for OVA peptide (323–339) was: 5′-

CCATCGATTCTGGTGGTTCTGCAGAGAGCCTGAAGATA-3′ and 5′-GGAATTCAGAACCACCAGATGACCCTACCACCTCTCT-3′ and the primer pair for OVA peptide (257–264) was: 5′-CCATCGATTCTGGTGGTTCTGATGAAGTCTCAGGCCTTGAGCA-3′ and 5′-GGAATTCAGAACCACCAGATTCCATAACATTAGAACTGG-3′. Both PCR products were cloned in-frame using *Cla*I/*Eco*RI digestion. 293T cells grown in protein-free media were transfected using FuGene HD transfection reagent (Roche). The transfection efficiency was ~60–70%, based on the percentage of $EGFP^+$ cells. Supernatants were collected, and the secreted fusion proteins were purified over Ni-NTA resin columns (Thermo Scientific) and eluted from the resin by increasing concentrations of imidazole (Acros organics) in buffer solutions. Eluted proteins were extensively dialyzed against PBS and quantitated by 10% SDS-PAGE followed by Coomassie blue staining, where BSA was used as a standard protein.

In vitro Ag presentation assay

cDCs, PDCs, monocytes, basophils, and B cells were isolated from OVAp-Fcε–injected hFcεRIα-Tg mice by FACS. Isolated cells (1×10^4 cells) were cultured with CTV (Invitrogen)-labeled $CD4^+$ OT-II T cells at a 1:5 APC/T cell ratio in a 96-well plate for 3 d. CTV dilution was analyzed by flow cytometry. When T cell proliferation was measured using ^{3}H-thymidine, isolated cells (5×10^3) were cocultured with $CD4^+$ OT-II T cells at a 1:10 APC/T cell ratio in a 96-well plate for 4 d. ^{3}H-thymidine was added for the last 15 h of the culture. As a positive control, $CD4^+$ OT-II T cells were incubated with 10 μg/ml anti-CD3 and 20 μg/ml anti-CD28 Abs (BD Biosciences).

In vivo Ag presentation assay

Indicated mice were injected i.v. with $0.5–1 \times 10^6$ CTV or CFSE-labeled Ag-specific $CD4^+$ or $CD8^+$ T cells. One day later, mice were injected i.v. with the indicated amounts of fusion proteins, OVA peptide (323–339; China peptides), or OVA protein (Fisher Scientific). Three, seven, or twelve days later, a single-cell suspension was prepared from spleen, lymph nodes, or blood, and stained for flow cytometry using fluorophore-labeled Abs directed against CD4, CD8, TCRVα2, and CD45.1.

In vivo Treg induction assay

Mice were injected i.v. with $0.5–1 \times 10^6$ CTV-labeled $CD4^+GFP^-$ T cells sorted from $Foxp3^{GFP}$OT-II mice expressing the congenic marker Thy1.1. One day later, mice were injected i.v. with OVAp-Fcε. Three, seven, or twelve days later, $CD4^+$ T cells were isolated from whole spleen by using anti-CD4 Ab magnetic beads (Stemcell Technologies), stained using fluorophore-labeled Abs directed against CD4, CD8, TCRVβ5, and Thy1.1, and analyzed by flow cytometry. $GFP^+CD4^+Thy1.1^+TCRVβ5^+$ cells were gated and cell numbers were determined.

T cell restimulation assay and delayed-type hypersensitivity assay

Naive $CD4^+$ T cells ($0.5–1 \times 10^6$) from OT-II mice were injected into hFcεRIα-Tg mice or Tg^- control mice. After 24 h, 0.5 μg OVAp-Fcε fusion proteins or PBS were injected. Seven

days later, mice were injected s.c. with 30 μg OVA peptide (323–339) mixed with IFA (Sigma). An additional 7 d later, mice were examined for the development of OVA-specific T cell immunity by performing the T cell restimulation assay and delayed-type hypersensitivity (DTH) assay. For the T cell restimulation assay, 2×10^5 splenocytes were isolated and incubated with or without 20 μg/ml OVA peptide (323–339) in a 96-well plate for 4 d. [^{3}H]Thymidine (1 μCi) was added to each well for the last 15 h of incubation. [^{3}H]Thymidine incorporated into cells was determined using Microbeta counter (1450 MicroBeta Trilux; PerkinElmer). For DTH assay, mice were injected onto the right footpads with 30 μg OVA peptide (323–339) mixed with IFA and onto the left footpads with IFA alone. Twenty-four hours later, thickness of each footpad was measured using a caliper rule.

Results

FcεRI is expressed on BDCA1$^+$ DCs, PDCs, monocytes, and basophils in human PBMCs

To determine which cells express FcεRI in human blood, we performed flow cytometry on human PBMCs using an anti-FcεRI Ab and a panel of cell type-specific Abs. We found that FcεRI was expressed on a small fraction of PBMCs and that this fraction was composed of more than one cell population, as indicated by heterogeneous labeling by FcεRI and CD14 Abs (Fig. 1A, *upper panel*). Further analysis revealed that these FcεRI-expressing cells consisted of basophils, plasmacytoid DCs (PDCs), BDCA1$^+$ DCs, and monocytes (Fig. 1A, *lower panel*). To confirm that these cell types indeed expressed FcεRI, we gated them independently of FcεRI expression using cell type–specific markers (Supplemental Fig. 1) and subsequently examined FcεRI expression. We found that BDCA1$^+$ DCs, PDCs, and basophils all expressed FcεRI homogeneously, whereas monocytes appeared to express it heterogeneously (Fig. 1B). We also examined BDCA3$^+$ DCs, T cells, B cells, and NK cells by gating them using specific markers (Supplemental Fig. 1). None of these cells expressed FcεRI at appreciable levels (Fig. 1B). Thus, FcεRI is specifically expressed in BDCA1$^+$ DCs, PDCs, basophils, and a subpopulation of monocytes in human PBMCs.

hFcεRIα-Tg mice have a similar pattern of hFcεRI expression compared with humans

To determine whether hFcεRIα-Tg mice express hFcεRI in a similar fashion to humans, we performed flow cytometry of blood cells from hFcεRIα-Tg mice using the same anti-human FcεRIα Ab. We found that basophils, monocytes, and PDCs expressed hFcεRI; cDCs also expressed it, although levels were significantly lower than for other cell types (Fig. 2A). No FcεRI was found on lymphocytes, including B cells (Fig. 2A). A similar expression profile of hFcεRI was found in the spleen (Fig. 2B). Thus, hFcεRIα-Tg mice express hFcεRI in cell types similar to humans, albeit with slightly different expression levels.

Generation of OVAp-Fcε recombinant protein

Having determined that hFcεRIα-Tg mice express hFcεRI similarly to humans, we decided to use these mice to examine whether IgE could be exploited to target Ags to DCs for presentation in vivo. For this study, we generated an OVAp-Fcε fusion protein. First, a cDNA was cloned encoding a V_k signal sequence linked sequentially to OVA peptide (323–339; OVAp), human IgE Cε2-Cε4 domains (Fcε), and 6XHis tag (Fig. 3A). In this study, the signal peptide was included to let the recombinant protein be secreted into the cell culture

media. OVA peptide (323–339) was included as a model Ag, the presentation of which can be readily determined by using OT-II transgenic mice, which express OVA-specific TCRs. The 6XHis tag was added to ease purification of recombinant protein via affinity chromatography. This cDNA construct was transfected into 293T cell lines cultured in protein-free media. Media was subsequently examined for the presence of the recombinant protein by using nonreducing SDS-PAGE followed by Western blot analysis using an anti-hIgE Ab and an anti-His Ab. A single protein band was detected at the m.w. of OVAp-Fcε dimers (Fig. 3D, 3E, "Supernatant"), which was expected because IgE heavy chains dimerize via intermolecular disulfide bonds (Fig. 3B) (29). To confirm dimerization, we ran the same sample on a reducing SDS-PAGE. As predicted, the reduced protein band appeared at about half the m.w. of the nonreduced protein band (Fig. 3F). We enriched and purified the recombinant protein by collecting media and running it through a Ni-NTA column. We found that the anti-IgE and anti-His reactive band was eluted from the column at high purity (Figs. 3C–3E, "Eluates").

Next, we determined whether OVAp-Fcε specifically binds to hFcεRI. OVAp-Fcε was incubated with U937 cells that were either untransfected or transfected with hFcεRI (27); flow cytometry was performed using an anti-hIgE Ab that specifically reacts with hIgE Fc domain. We found that anti-hIgE Ab stained hFcεRI-transfected U937 cells but not untransfected cells (Fig. 3G), indicating that OVAp-Fcε specifically binds to FcεRI. We also determined whether OVAp-Fcε cross-links FcεRI. OVAp-Fcε was incubated with hFcεRIα-Tg mouse bone marrow–derived mast cells, and degranulation was quantified by hexosaminidase release assay (30). No hexosaminidase was released upon incubation with the construct (Supplemental Fig. 2), indicating that OVAp-Fcε does not cross-link FcεRI.

OVAp-Fcε binds to human DCs in vitro and to DCs of hFcεRIα-Tg mice in vivo

Next, we examined whether OVAp-Fcε binds to human DCs. OVAp-Fcε was incubated with human PBMCs, and its binding to cells was determined by flow cytometry with an anti-His Ab to avoid unintentional signal from endogenous IgE bound to FcεRI. We found that anti-His Ab bound to all FcεRI-expressing cells, including BDCA1$^+$ DCs, PDCs, basophils, and monocytes, but not to FcεRI-nonexpressing cells such as BDCA3$^+$ DCs (Fig. 4A). This finding indicates that OVAp-Fcε specifically binds to human DCs and other FcεRI-expressing cells.

Next, we examined whether OVAp-Fcε binds to DCs of hFcεRIα-Tg mice in vivo. OVAp-Fcε was injected i.v. into hFcεRIα-Tg mice. One hour after injection, we isolated blood cells and performed flow cytometry using anti-His Ab and cell type specific Abs. We found that anti-His Ab bound to cDCs and other hFcεRI-expressing cells such as PDCs, but not to FcεRI-negative cells such as B cells (Fig. 4B, *upper panel*). Like in blood, anti-His Ab stained cDCs and other hFcεRI-expressing cells, but not B cells in the spleen (Fig. 4C). To confirm that OVAp-Fcε binding to DCs is mediated by hFcεRI, we performed the same experiment using Tg-negative control mice and found no anti-His Ab binding in any cell types (Fig. 4B, *lower panel*). Thus, OVAp-Fcε binds to DCs in hFcεRIα-Tg mice in an hFcεRI-dependent manner.

Ag targeting to hFcεRI enhances Ag presentation in hFcεRIα-Tg mice by 1000–2500 fold in vivo

To determine whether Ag targeted to FcεRI through our Ag-Fcε fusion protein is presented in vivo, we injected OVAp-Fcε into hFcεRIα-Tg mice that had been adoptively transferred with a mixture of CTV-labeled OT-II and CFSE-labeled SMARTA mouse $CD4^+$ T cells. We included SMARTA T cells, which are specific for an irrelevant Ag, to determine whether T cell proliferation is Ag-specific or whether it is the result of nonspecific T cell activation. Proliferation of OT-II and SMARTA $CD4^+$ T cells was examined 3 d after OVAp-Fcε injection by determining the dilution of CFSE and CTV by flow cytometry. As expected, dilution of CTV was readily detected while dilution of CFSE was not observed (Fig. 5A). This finding indicates that Ag targeted to FcεRI through Ag-Fcε fusion protein is presented to Ag-specific T cells in hFcεRIα-Tg mice, resulting in the restricted proliferation of only Ag-specific cells.

Next, we examined the degree to which targeting Ags to FcεRI enhances Ag presentation. For this study, CTV-labeled OT-II $CD4^+$ T cells were transferred into hFcεRIα-Tg and Tg^- control mice. One day later, mice were injected i.v. with 0.05–0.5 μg OVAp-Fcε. Spleens were harvested 3 d later, and the dilution of CTV was examined by flow cytometry. We found that OTII $CD4^+$ T cells proliferated in hFcεRIα-Tg mice, but not in control mice (Fig. 5B). To determine whether the lack of OT-II T cell proliferation in control mice is due to a general defect in Ag processing or presentation of these mice, we injected hFcεRIα-Tg mice and non-Tg control mice with OVA Ags at high doses, such as 10 μg OVA peptide (323–339) or 50 μg OVA protein. We found that OT-II $CD4^+$ T cells proliferated in control mice and hFcεRIα-Tg mice to a similar degree (Fig. 5C, 5D), indicating that Ag processing and presentation are not significantly different between Tg^+ and Tg^- mice. Thus, it is the targeting of OVA to FcεRI that dramatically enhances OTII T cell proliferation.

To quantify the increase in Ag presentation efficiency when Ags were targeted to FcεRI via IgE, we compared the degree of OT-II T cell proliferation in hFcεRIα-Tg mice injected with OVAp-Fcε versus OVA protein or peptide (323–339). We found that 0.1 μg OVAp-Fcε (which contains an equivalent molar quantity of 0.004 μg OVA peptide [323–339]) induced OTII T cell proliferation to a degree similar to 10 μg of OVA peptide (323–339; Fig. 5E), and that 0.05 μg of OVAp-Fcε elicited an OT-II T cell proliferation equivalent to that of 50 μg OVA protein (Fig. 5F). These findings indicate that Ag presentation increases by 1000–2500 fold when Ag is targeted to FcεRI in hFcεRIα-Tg mice.

It is noteworthy that targeting Ags to FcεRI did not appear to enhance Ag presentation to $CD8^+$ T cells. We generated OVA (257–264)-Fcε and injected it into hFcεRIα-Tg and Tg^- control mice that had received OT-I $CD8^+$ T cells expressing OVA (257–264)-specific TCR. We found that OT-I $CD8^+$ T cells proliferated in Tg^+ and Tg^- mice to similar degrees (Supplemental Fig. 3), indicating that DC targeting of Ags via FcεRI only enhances Ag presentation to $CD4^+$ T cells in this mouse model.

FcεRI-targeted Ags are specifically presented by cDCs in hFcεRIα-Tg mice

To investigate which FcεRI-expressing cells present OVA targeted to FcεRI, we i.v. injected hFcεRI Tg-mice with OVAp-Fcε. After 24 h, cDCs, PDCs, basophils, monocytes, and B cells were isolated from spleen by FACS. Each of the isolated cell types was cultured with CTV-labeled OT-II $CD4^+$ T cells, and the dilution of CTV was determined by flow cytometry 4 d later. We found that dilution of CTV was limited to when OT-II $CD4^+$ T cells were cultured with cDCs, although the extent of proliferation was markedly weaker that what was seen in vivo (Fig. 6A). This weak proliferation is likely due to low number of APCs used in this assay because of the scarcity of basophils in spleens. Nevertheless, quantification of data from three independent experiments indicated that cDCs, but no other cell type, induced OT-II proliferation at significant levels (Fig. 6B). We also performed the [^{3}H]thymidine uptake, which is perhaps more sensitive and quantitative than CTV dilution assay. As shown in Fig. 6C, [^{3}H]thymidine was incorporated into OT-II T cells incubated with cDCs, but not any other APCs. These findings indicate that although cDCs, PDCs, basophils, and monocytes all express FcεRI and bind OVAp-Fcε in hFcεRIα-Tg mice (Figs. 2, 4), cDCs are the only cells that present OVA.

Ag targeting to FcεRI results in Ag-specific $CD4^+$ T cell deletion in hFcεRIα-Tg mice

Next, we examined the fate of OT-II $CD4^+$ T cells following proliferation in hFcεRIα-Tg mice injected with OVAp-Fcε. For this study, we adoptively transferred CD45.1 expressing CTV-labeled OT-II $CD4^+$ T cells into hFcεRIα-Tg mice, injected the mice i.v. with OVAp-Fcε the following day, and determined the frequency and CTV dilution of $CD45.1^+$ cells in the spleen at days 3, 7, and 12 after injection. We observed substantial dilution of CTV on day 3, indicating OT-II $CD4^+$ T cell proliferation. However, proliferation did not continue; in fact, there were fewer $CD45.1^+$ cells observed on day 7, and they completely disappeared by day 12 (Fig. 7A). When we quantitated the frequency of $CD45.1^+$ cells in the spleen, lymph node, and blood, we found that these cells were disappearing over time from all these organs, indicating systemic deletion (Fig. 7B). To determine whether hFcεRIα-Tg mice have an intrinsic defect in expanding Ag-specific T cells, we examined OT-II $CD4^+$ T cell expansion in these mice after injection of OVAp-Fcε together with the immunostimulatory agent LPS. We found that OT-II $CD4^+$ T cells proliferated substantially and continuously for the entire 12 d of examination in spleen, LN, and blood (Fig. 7C, 7D). This finding indicates that hFcεRIα-Tg mice are capable of expanding Ag-specific T cells when Ag is targeted to hFcεRI in the presence of inflammatory stimuli, but delete them when Ag is targeted to hFcεRI in the absence of such stimuli.

We also examined whether targeting Ags to hFcεRI induces Ag-specific regulatory T cells (Tregs) in hFcεRIα-Tg mice. Mice were adoptively transferred with GFP^-CD4^+ T cells that were isolated from Foxp3^{GFP}OT-II mice by FACS (Fig. 8A) and labeled with CTV. OVAp-Fcε was injected i.v. the next day, and GFP expression by transferred OT-II $CD4^+$ T cells was monitored by flow cytometry. Very few GFP^+OT-II $CD4^+$ cells were found at any days of examination following injection with OVAp-Fcε at high or low doses (Fig. 8B, 8C). Thus, Ag-targeting to hFcεRI hardly induces Tregs.

Ag-Fcε fusion protein inhibits development of Ag-specific T cell immunity in FcεRIα-Tg mice

Lastly, we investigated whether targeting Ags to FcεRI could inhibit development of Ag-specific T cell immunity and induce T cell tolerance in vivo. For this study, we examined whether OVAp-Fcε could prevent hFcεRIα-Tg mice from developing delayed-type hypersensitivity against OVA. hFcεRIα-Tg mice adoptively transferred with OT-II $CD4^+$ T cells were injected i.v. with either OVAp-Fcε or PBS. Seven days later, mice were immunized with OVA peptide mixed with IFA. An additional 7 d later, OVA-specific T cell immunity was determined using either in vitro restimulation assay or DTH assay. For the in vitro re-stimulation assay, splenocytes were isolated from mice, incubated with OVA peptide, and examined for proliferation using [^{3}H]thymidine. We found that cells from OVAp-Fcε–injected mice incorporated [^{3}H]thymidine at significantly lower levels than cells from PBS-injected mice did. This finding indicates that OVAp-Fcε inhibits the development of OVA-specific T cell immunity in hFcεRIα-Tg mice (Fig. 9B). To verify that this inhibitory effect was mediated by hFcεRI, the same experiment was performed using control mice that do not express hFcεRI. Splenocytes from OVAp-Fcε–injected control mice incorporated [^{3}H]thymidine as much as those from PBS-injected hFcεRIα-Tg mice did (Fig. 9B). Thus, OVAp-Fcε inhibits development of OVA-specific T cell immunity only when hFcεRI is expressed.

For DTH assay, mice were injected into the left footpads with OVA peptide mixed with IFA, and into the right footpads with IFA alone. Twenty-four hours after injection, the thickness of each footpad was measured. The thickness of the left footpad was subtracted from that of the right footpad to determine swelling induced by OVA rechallenge (Fig. 8A). We found that both PBS and OVAp-Fcε–injected mice showed appreciable swelling, but the degree was markedly less in OVAp-Fcε–injected mice, suggesting that OVAp-Fcε injection significantly inhibited mice from developing DTH (Fig. 8C). Importantly, OVAp-Fcε failed to inhibit Tg^- control mice from developing DTH (Fig. 8C) indicating that the inhibitory effect of OVAp-Fcε in DTH development requires hFcεRI expression. Taken together, these findings demonstrate that Ag targeting to FcεRI inhibits the development of Ag-specific T cell immunity and induces T cell tolerance.

Discussion

In this study, we have found that Ag-Fcε fusion proteins can be exploited to target Ags to DCs and induce Ag-specific T cell tolerance. We found that Ag-Fcε bound to human DCs in vitro and to DCs of hFcεRIα-Tg mice in vivo, and that injection of hFcεRIα-Tg mice with Ag-Fcε resulted in Ag presentation by DCs and subsequent systemic deletion of Ag-specific T cells. Importantly, injection of Ag-Fcε into hFcεRIα-Tg mice significantly inhibited these mice from developing DTH.

Previous studies have indicated that the efficiency of Ag presentation can be increased by 100–1000 fold when Ags are conjugated with DC-specific Abs such as anti-DEC-205, DECTIN-1, DNGR1, DCIR, Langerin, Treml4, or DC-SIGN (9, 14, 31–33). We found in hFcεRIα-Tg mice that Ags conjugated with human Fcε were presented by DCs at 1000–2500 fold higher efficiency than unconjugated Ags were. We predict that the efficiency of

targeting of this construct to human DCs will be even higher than in hFcεRIα-Tg mice, because human DCs express much higher levels of FcεRI than hFcεRIα-Tg mouse DCs do. Thus, the efficiency of Ag presentation in humans may increase markedly when Ags are conjugated with Fcε than when it is conjugated with DC-specific Ab. In addition, generation of Ag-Fcε fusion protein is more straightforward, as described in this study, and perhaps more cost-effective than the generation of Ag-DC-specific Ab fusion protein. A single cDNA cloning and transfection will generate Ag-Fcε; there is no need to immunize animals, generate and select hybridomas, and humanize selected Abs.

The mechanism by which Fcε-linked Ag is presented to $CD4^+$ T cells remains to be determined. It has been known that IgE/FcεRI cross-linking using multivalent Ags results in the entry of Ag/IgE/FcεRI complexes to endocytic compartments in DCs and subsequent processing and presentation of the Ags to $CD4^+$ T cells (34, 35). However, whether non–cross-linking Ag could follow the same pathway of DC entry has never been examined. Our finding that Fcε-linked Ag, which binds to FcεRI on DCs without cross-linking it, is presented to $CD4^+$ T cells strongly suggests that cross-linking is not required for IgE/FcεRI entry to DC endosomal compartments. Some other work in our laboratory indicates significant amounts of IgE and FcεRI localized in endolysosomal compartments in $BDCA1^+$ DCs freshly isolated from human blood and DCs from hFcεRIα-Tg mice (unpublished observations). Because DCs do not make IgE themselves, the presence of IgE and FcεRI in the endolysosomal compartment implies that FcεRI traffics through endocytic pathway in DCs at steady state and that IgE enters DCs by binding to FcεRI at cell surface. Ag-Fcε is likely to follow the same pathway of entry.

Ag targeting to DCs in the absence of DC maturation stimuli has been proposed to induce T cell unresponsiveness, deletion, or conversion to Tregs (9, 36–38). Accordingly, we found that targeting Ags to FcεRI via Ag-Fcε fusion protein results in T cell deletion in hFcεRIα-Tg mice. Ag-Fcε binding to FcεRI is unlikely to activate DCs, mast cells, or basophils because it does not cross-link FcεRI. Consistently, no degranulation was observed when mast cells were incubated with Ag-Fcε. Thus, Ag presentation in these mice is likely to have been mediated by steady state immature DCs, which may then facilitate Ag-specific T cell deletion. Indeed, when the DC maturation stimulus LPS was coinjected with OVAp-Fcε into hFcεRIα-Tg mice, OVA-specific T cells expanded and persisted over 12 d after injection, supporting the important contribution of DC activation status to T cell fate determination. Few Ag-specific Tregs were observed in our study, although others have found robust Treg induction when Ag was targeted to DEC-205 or Langerin (14, 37). Possibly, injection of OVAp-Fcε into the peripheral tissue sites rather than blood induced Treg cells, because these cells appear to be better generated by peripheral tissue migratory DCs (14).

DTH response is commonly examined to assess T cell–mediated immunity in vivo. A lack of DTH response to a recall Ag is regarded as an evidence of deficiency in primary T cell immunity. We found that OVAp-Fcε injection i.v. markedly inhibited hFcεRIα-Tg mice from developing OVA-specific DTH and that this inhibitory effect was completely dependent on the expression of hFcεRI in these mice. This finding strongly suggests that human FcεRI-targeted Ag is capable of undermining primary T cell immunity and developing Ag-specific tolerance in vivo. We intend to test in the near future whether

injection of hFcεRIα-Tg mice with a self-antigen– or allergen-linked Fcε makes these mice resistant to autoimmune or allergic diseases.

In conclusion, this study proposes a novel approach to target Ags to human DCs for the induction of Ag-specific tolerance. Further studies on its efficacy, mechanism, and clinical safety may lead to the development of new therapeutics.

Supplementary Material

Refer to Web version on PubMed Central for supplementary material.

Acknowledgments

We thank Dr. Amy Putnam for blood drawing, Dr. Jean-Pierre Kinet for the hFcεRIα-Tg mice and U937 cells, Drs. Dirk Baumjohann and Laurence Cheng for helping with mice and cDNA construct, and Dr. Bithi Chatterjee for critical reading of the manuscript.

This work was supported by funding from the University of California San Francisco (UCSF) Resource Allocation Program (to J-S.S.), the American Heart Association (to J-S.S.), and the UCSF Sandler Asthma Basic Research Center.

Abbreviations used in this article

cDC	conventional dendritic cell
DC	dendritic cell
DTH	delayed-type hypersensitivity
NOD	nonobese diabetic
PDC	plasmacytoid dendritic cell
Treg	regulatory T cell
UCSF	University of California San Francisco

References

1. Steinman RM, Hawiger D, Nussenzweig MC. Tolerogenic dendritic cells. Annu Rev Immunol. 2003; 21:685–711. [PubMed: 12615891]
2. Ohnmacht C, Pullner A, King SB, Drexler I, Meier S, Brocker T, Voehringer D. Constitutive ablation of dendritic cells breaks self-tolerance of CD4 T cells and results in spontaneous fatal autoimmunity. J Exp Med. 2009; 206:549–559. [PubMed: 19237601]
3. Belz GT, Behrens GM, Smith CM, Miller JF, Jones C, Lejon K, Fathman CG, Mueller SN, Shortman K, Carbone FR, Heath WR. The CD8alpha(+) dendritic cell is responsible for inducing peripheral self-tolerance to tissue-associated antigens. J Exp Med. 2002; 196:1099–1104. [PubMed: 12391021]
4. Scheinecker C, McHugh R, Shevach EM, Germain RN. Constitutive presentation of a natural tissue autoantigen exclusively by dendritic cells in the draining lymph node. J Exp Med. 2002; 196:1079–1090. [PubMed: 12391019]
5. Wilson NS, El-Sukkari D, Villadangos JA. Dendritic cells constitutively present self antigens in their immature state in vivo and regulate antigen presentation by controlling the rates of MHC class II synthesis and endocytosis. Blood. 2004; 103:2187–2195. [PubMed: 14604956]

6. Probst HC, Lagnel J, Kollias G, van den Broek M. Inducible transgenic mice reveal resting dendritic cells as potent inducers of CD8+ T cell tolerance. Immunity. 2003; 18:713–720. [PubMed: 12753747]
7. Maksimow M, Miiluniemi M, Marttila-Ichihara F, Jalkanen S, Hänninen A. Antigen targeting to endosomal pathway in dendritic cell vaccination activates regulatory T cells and attenuates tumor immunity. Blood. 2006; 108:1298–1305. [PubMed: 16621963]
8. Proietto AI, van Dommelen S, Zhou P, Rizzitelli A, D'Amico A, Steptoe RJ, Naik SH, Lahoud MH, Liu Y, Zheng P, et al. Dendritic cells in the thymus contribute to T-regulatory cell induction. Proc Natl Acad Sci USA. 2008; 105:19869–19874. [PubMed: 19073916]
9. Hawiger D, Inaba K, Dorsett Y, Guo M, Mahnke K, Rivera M, Ravetch JV, Steinman RM, Nussenzweig MC. Dendritic cells induce peripheral T cell unresponsiveness under steady state conditions in vivo. J Exp Med. 2001; 194:769–779. [PubMed: 11560993]
10. Bonifaz L, Bonnyay D, Mahnke K, Rivera M, Nussenzweig MC, Steinman RM. Efficient targeting of protein antigen to the dendritic cell receptor DEC-205 in the steady state leads to antigen presentation on major histocompatibility complex class I products and peripheral CD8+ T cell tolerance. J Exp Med. 2002; 196:1627–1638. [PubMed: 12486105]
11. Mukhopadhaya A, Hanafusa T, Jarchum I, Chen YG, Iwai Y, Serreze DV, Steinman RM, Tarbell KV, DiLorenzo TP. Selective delivery of beta cell antigen to dendritic cells in vivo leads to deletion and tolerance of autoreactive CD8+ T cells in NOD mice. Proc Natl Acad Sci USA. 2008; 105:6374–6379. [PubMed: 18430797]
12. Petzold C, Riewaldt J, Koenig T, Schallenberg S, Kretschmer K. Dendritic cell-targeted pancreatic beta-cell antigen leads to conversion of self-reactive CD4(+) T cells into regulatory T cells and promotes immunotolerance in NOD mice. Rev Diabet Stud. 2010; 7:47–61. [PubMed: 20703438]
13. Hawiger D, Masilamani RF, Bettelli E, Kuchroo VK, Nussenzweig MC. Immunological unresponsiveness characterized by increased expression of CD5 on peripheral T cells induced by dendritic cells in vivo. Immunity. 2004; 20:695–705. [PubMed: 15189735]
14. Idoyaga J, Fiorese C, Zbytnuik L, Lubkin A, Miller J, Malissen B, Mucida D, Merad M, Steinman RM. Specialized role of migratory dendritic cells in peripheral tolerance induction. J Clin Invest. 2013; 123:844–854. [PubMed: 23298832]
15. Kato M, McDonald KJ, Khan S, Ross IL, Vuckovic S, Chen K, Munster D, MacDonald KP, Hart DN. Expression of human DEC-205 (CD205) multilectin receptor on leukocytes. Int Immunol. 2006; 18:857–869. [PubMed: 16581822]
16. Murray EW, Robbins SM. Antibody cross-linking of the glycosylphosphatidylinositol-linked protein CD59 on hematopoietic cells induces signaling pathways resembling activation by complement. J Biol Chem. 1998; 273:25279–25284. [PubMed: 9737993]
17. Rintoul RC, Buttery RC, Mackinnon AC, Wong WS, Mosher D, Haslett C, Sethi T. Cross-linking CD98 promotes integrin-like signaling and anchorage-independent growth. Mol Biol Cell. 2002; 13:2841–2852. [PubMed: 12181350]
18. Nam KO, Kang H, Shin SM, Cho KH, Kwon B, Kwon BS, Kim SJ, Lee HW. Cross-linking of 4-1BB activates TCR-signaling pathways in CD8+ T lymphocytes. J Immunol. 2005; 174:1898–1905. [PubMed: 15699116]
19. Rothlein R, Kishimoto TK, Mainolfi E. Cross-linking of ICAM-1 induces co-signaling of an oxidative burst from mononuclear leukocytes. J Immunol. 1994; 152:2488–2495. [PubMed: 7510744]
20. Ramakrishna V, Treml JF, Vitale L, Connolly JE, O'Neill T, Smith PA, Jones CL, He LZ, Goldstein J, Wallace PK, et al. Mannose receptor targeting of tumor antigen pmel17 to human dendritic cells directs anti-melanoma T cell responses via multiple HLA molecules. J Immunol. 2004; 172:2845–2852. [PubMed: 14978085]
21. Kraft S, Kinet JP. New developments in FcepsilonRI regulation, function and inhibition. Nat Rev Immunol. 2007; 7:365–378. [PubMed: 17438574]
22. Garman SC, Wurzburg BA, Tarchevskaya SS, Kinet JP, Jardetzky TS. Structure of the Fc fragment of human IgE bound to its high-affinity receptor Fc epsilonRI alpha. Nature. 2000; 406:259–266. [PubMed: 10917520]

23. Bax HJ, Keeble AH, Gould HJ. Cytokinergic IgE Action in Mast Cell Activation. Front Immunol. 2012; 3:229. [PubMed: 22888332]
24. Dombrowicz D, Lin S, Flamand V, Brini AT, Koller BH, Kinet JP. Allergy-associated FcRbeta is a molecular amplifier of IgE- and IgG-mediated in vivo responses. Immunity. 1998; 8:517–529. [PubMed: 9586641]
25. Oxenius A, Bachmann MF, Zinkernagel RM, Hengartner H. Virus-specific MHC-class II-restricted TCR-transgenic mice: effects on humoral and cellular immune responses after viral infection. Eur J Immunol. 1998; 28:390–400. [PubMed: 9485218]
26. Fontenot JD, Rasmussen JP, Williams LM, Dooley JL, Farr AG, Rudensky AY. Regulatory T cell lineage specification by the forkhead transcription factor foxp3. Immunity. 2005; 22:329–341. [PubMed: 15780990]
27. Donnadieu E, Jouvin MH, Kinet JP. A second amplifier function for the allergy-associated Fc(epsilon)RI-beta subunit. Immunity. 2000; 12:515–523. [PubMed: 10843384]
28. Kanof, ME.; Smith, PD.; Zola, H. Isolation of whole mononuclear cells from peripheral blood and cord blood. In: Coligan, JE.; Bierer, B.; Margulies, DH.; Shevach, EM.; Strober, W.; Brown, P.; Donovan, JC.; Kruisbeek, AM., editors. Current Protocols in Immunology. Vol. Chapter 7. John Wiley & Sons; Hoboken, NJ: 2001.
29. Takatsu K, Ishizaka T, Ishizaka K. Biologic significance of disulfide bonds in human IgE molecules. J Immunol. 1975; 114:1838–1845. [PubMed: 47881]
30. Shin JS, Shelburne CP, Jin C, LeFurgey EA, Abraham SN. Harboring of particulate allergens within secretory compartments by mast cells following IgE/FcepsilonRI-lipid raft-mediated phagocytosis. J Immunol. 2006; 177:5791–5800. [PubMed: 17056503]
31. Carter RW, Thompson C, Reid DM, Wong SY, Tough DF. Preferential induction of CD4+ T cell responses through in vivo targeting of antigen to dendritic cell-associated C-type lectin-1. J Immunol. 2006; 177:2276–2284. [PubMed: 16887988]
32. Sancho D, Mourão-Sá D, Joffre OP, Schulz O, Rogers NC, Pennington DJ, Carlyle JR, Reis e Sousa C. Tumor therapy in mice via antigen targeting to a novel, DC-restricted C-type lectin. J Clin Invest. 2008; 118:2098–2110. [PubMed: 18497879]
33. Engering A, Geijtenbeek TB, van Vliet SJ, Wijers M, van Liempt E, Demaurex N, Lanzavecchia A, Fransen J, Figdor CG, Piguet V, van Kooyk Y. The dendritic cell-specific adhesion receptor DC-SIGN internalizes antigen for presentation to T cells. J Immunol. 2002; 168:2118–2126. [PubMed: 11859097]
34. Maurer D, Fiebiger S, Ebner C, Reininger B, Fischer GF, Wichlas S, Jouvin MH, Schmitt-Egenolf M, Kraft D, Kinet JP, Stingl G. Peripheral blood dendritic cells express Fc epsilon RI as a complex composed of Fc epsilon RI alpha- and Fc epsilon RI gamma-chains and can use this receptor for IgE-mediated allergen presentation. J Immunol. 1996; 157:607–616. [PubMed: 8752908]
35. Maurer D, Fiebiger E, Reininger B, Ebner C, Petzelbauer P, Shi GP, Chapman HA, Stingl G. Fc epsilon receptor I on dendritic cells delivers IgE-bound multivalent antigens into a cathepsin S-dependent pathway of MHC class II presentation. J Immunol. 1998; 161:2731–2739. [PubMed: 9743330]
36. Dudziak D, Kamphorst AO, Heidkamp GF, Buchholz VR, Trumpfheller C, Yamazaki S, Cheong C, Liu K, Lee HW, Park CG, et al. Differential antigen processing by dendritic cell subsets in vivo. Science. 2007; 315:107–111. [PubMed: 17204652]
37. Kretschmer K, Apostolou I, Hawiger D, Khazaie K, Nussenzweig MC, von Boehmer H. Inducing and expanding regulatory T cell populations by foreign antigen. Nat Immunol. 2005; 6:1219–1227. [PubMed: 16244650]
38. Yamazaki S, Bonito AJ, Spisek R, Dhodapkar M, Inaba K, Steinman RM. Dendritic cells are specialized accessory cells along with TGF- for the differentiation of Foxp3+ CD4+ regulatory T cells from peripheral Foxp3 precursors. Blood. 2007; 110:4293–4302. [PubMed: 17699744]

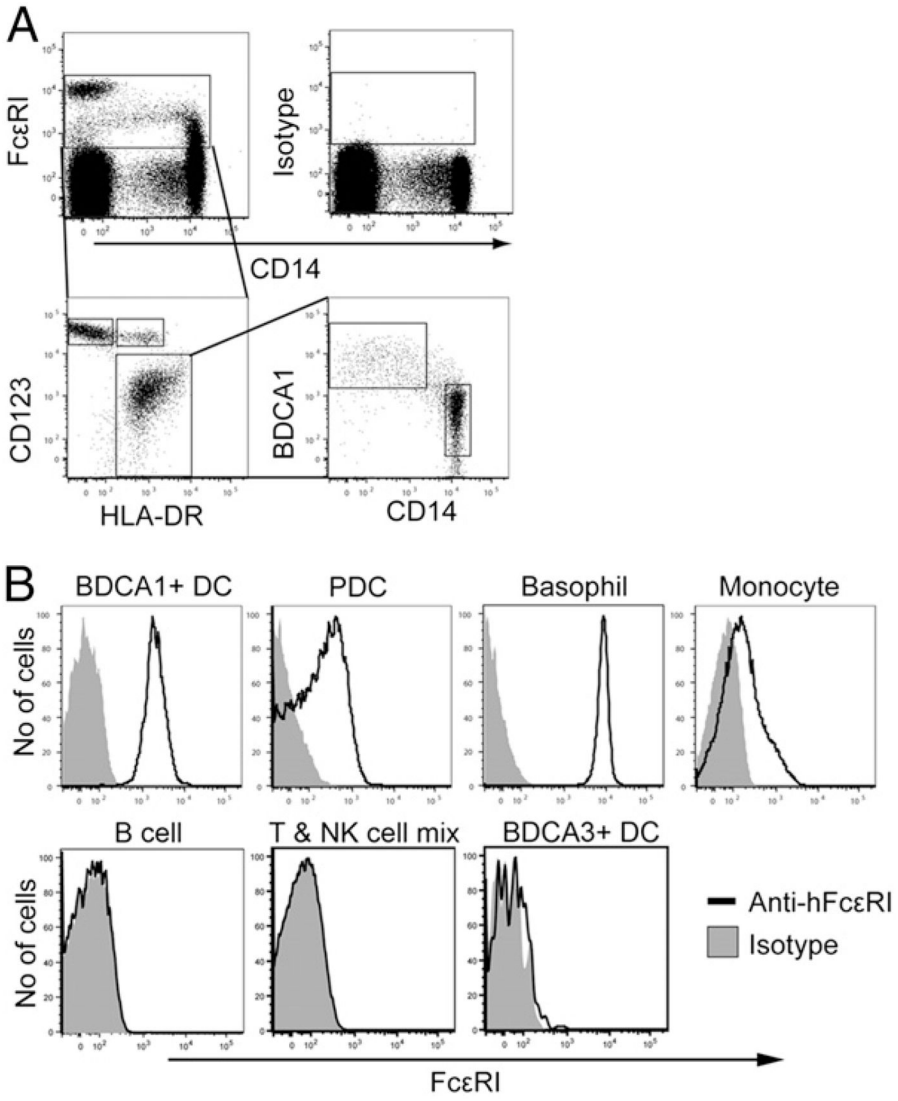

FIGURE 1.

FcεRI is expressed on BDCA1$^+$ DCs, PDCs, monocytes, and basophils among human PBMCs. (**A**) Identification of FcεRI-expressing cells in human PBMCs by flow cytometry. PBMCs were isolated from healthy blood donors and stained with a panel of cell-identification Abs (anti-CD14, HLA-DR, BDCA1, CD123, CD3, CD19, and CD56) and FcεRIα or isotype control Ab. (**B**) FcεRI expression in human blood BDCA1$^+$ DCs, PDCs, basophils, and monocytes, but not BDCA3$^+$ DCs, B cells, T cells, or NK cells. PBMCs were stained as described in (A) and gated by flow cytometry as shown in Supplemental Fig. 1. Anti-hFcεRIα Ab staining is shown black, and isotype control Ab staining is shown gray. Data are representative of three independent experiments with blood collected from multiple donors.

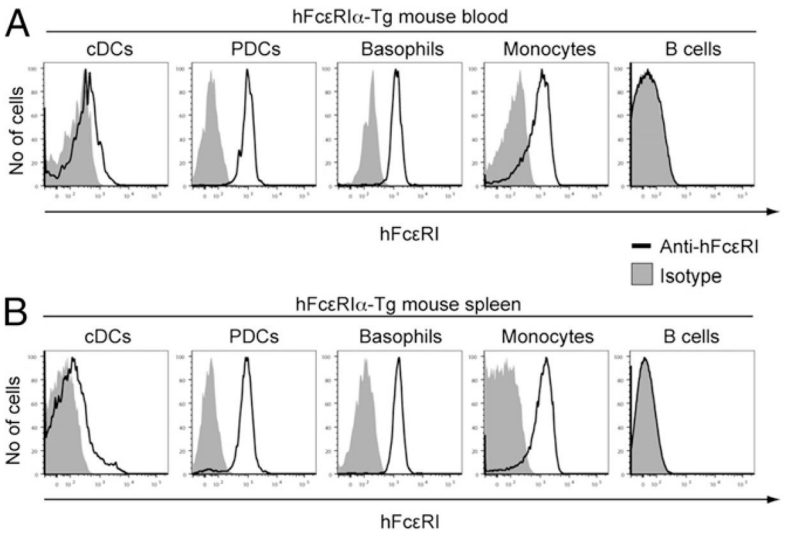

FIGURE 2.

hFcεRIα-Tg mice show hFcεRI expression pattern similar to those in humans. Expression of hFcεRI in hFcεRIα-Tg mouse blood (**A**) and spleen (**B**). Blood leukocytes and splenocytes were isolated from hFcεRIα-Tg mice and stained using cell-identification Abs (anti-CD11c, MHCII, Dx5, CD131, CD11b, GR1, and mPDCA1) and hFcεRIα or isotype control Ab. Cells were gated as described in *Materials and Methods*. Anti-FcεRIα Ab staining is shown black, and isotype control Ab staining is shown gray. Data are representative of five independent experiments.

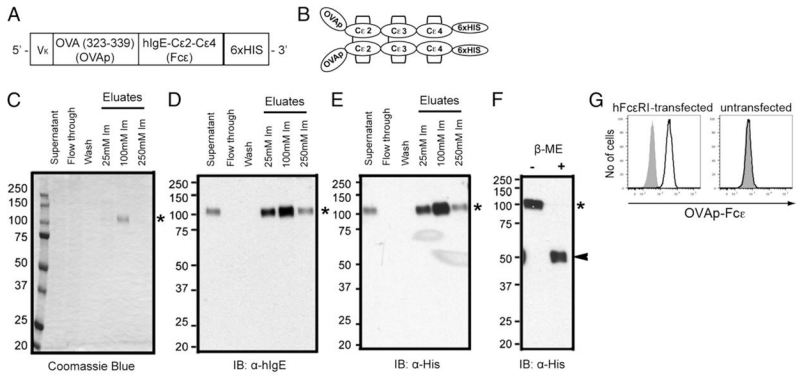

FIGURE 3.

Generation of OVAp-Fcε recombinant protein. (**A**) A schematic diagram of OVAp-Fcε cDNA. The $V_{k\ (\kappa)}$ signal sequence cDNA is positioned at the 5′ terminal end of an extended sequence containing OVA peptide (323–339; OVAp) linked to the Cε2-Cε4 domains of hIgE with a 6XHis tag cDNA at the 3′ terminal end. (**B**) A schematic diagram of OVAp-Fcε recombinant protein. Disulfide bonds predicted to form intramolecularly and intermolecularly are indicated by ∩ and |, respectively. (**C**–**F**) Generation and purification of OVAp-Fcε. OVAp-Fcε cDNA—shown in (A)—was transfected into 293T cells cultured in serum-free media. OVAp-Fcε was purified via Ni-NTA column chromatography via Imidazole (Im) elution. Culture supernatant and the chromatography fractions were both analyzed with nonreducing SDS-PAGE (C) followed by immunoblotting (IB) (D and E). Culture supernatant was also analyzed with a reducing SDS-PAGE (F). Nonreducing and reducing SDS-PAGE was labeled as β-mercaptoethanol (β-ME) – and +, respectively. An asterisk and an arrowhead indicate the nonreduced and reduced OVAp-Fcε, respectively. (**G**) Binding of OVAp-Fcε to hFcεRI determined by flow cytometry. hFcεRI-transfected (*left panel*) and untransfected U937 cells (*right panel*) were incubated with 1 μg/ml OVAp-Fcε at 37°C for 1 h, and stained with anti-hIgE Ab (black) or isotype control Ab (gray). Experiments shown in (C)–(G) were performed at least three times.

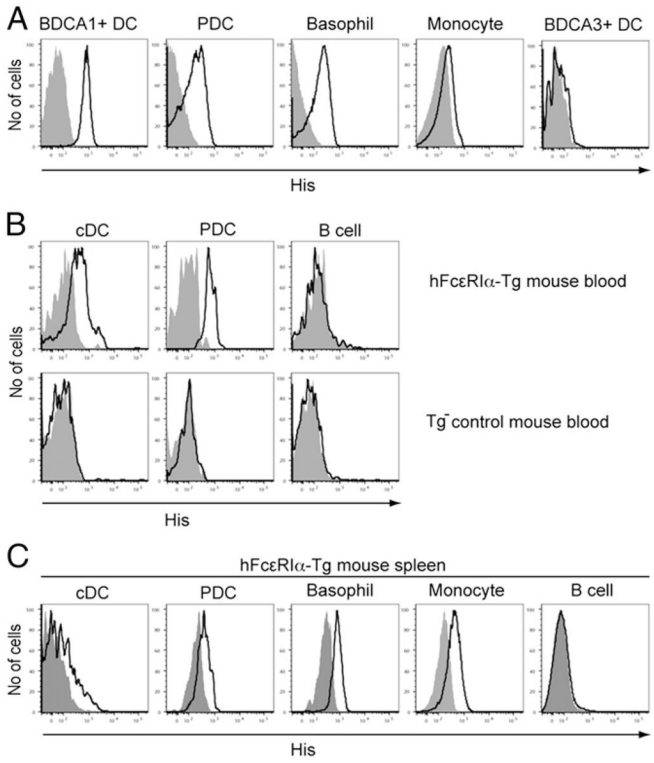

FIGURE 4.

OVAp-Fcε binds to human DCs in vitro and to DCs of hFcεRIα-Tg mice in vivo. (**A**) OVAp-Fcε binding to human DCs in vitro. Human PBMCs were incubated with 1 μg/ml OVAp-Fcε at 37°C for 1 h, washed, stained using cell type specific Abs and anti-His (Penta) or isotype control Ab, and analyzed by flow cytometry. Shown is the binding of anti-His (Penta) Ab (black) compared with isotype control Ab (gray) to each cell type. **(B)** OVAp-Fcε binding to DCs of hFcεRIα-Tg mice in vivo. hFcεRIα-Tg mice (*upper panel*) or Tg^{-} control mice (*lower panel*) were injected i.v. with 0.6 μg OVAp-Fcε. One hour later, blood leukocytes were isolated, stained using cell type–specific Abs and anti-His (Penta) or isotype control Ab, and analyzed by flow cytometry. Shown is the binding of anti-His (Penta) Ab (black) compared with isotype control Ab (gray) to specific cell types. (**C**) hFcεRIα-Tg mice were injected i.v. with 0.6 μg OVAp-Fcε. Five hour later, spleens were harvested and single-cell suspensions were stained and analyzed as described in Figs. 2 and 4B. Shown is the binding of anti-His (Penta) Ab (black) compared with isotype control Ab (gray) to specific cell types. All data shown in (A)–(C) are representative of three or four independent experiments.

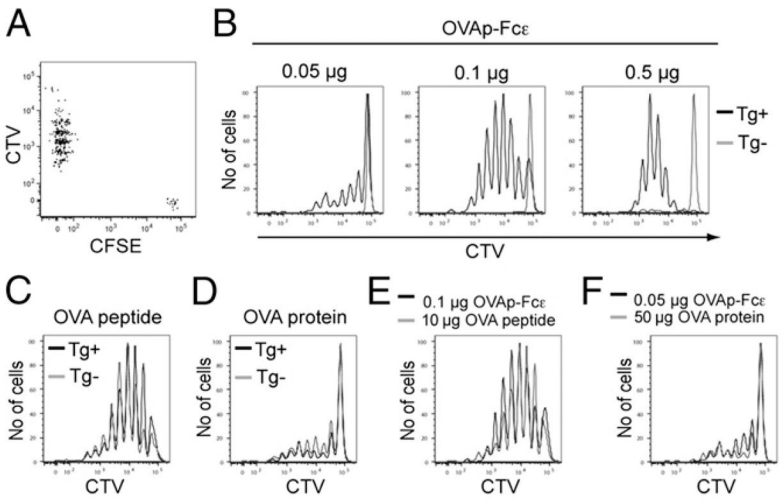

FIGURE 5.

Ag targeting to hFcεRI enhances Ag presentation in hFcεRIα-Tg mice by 1000–2500 fold. (**A**) OVA presentation in hFcεRIα-Tg mice injected with OVAp-Fcε. hFcεRIα-Tg mice were adoptively transferred with CTV (Cell Trace Violet)-labeled $CD45.1^+CD4^+$ OT-II T cells and CFSE-labeled $CD45.1^+CD4^+$ SMARTA T cells at equal numbers 1 d before i.v. injection with 0.2 μg OVAp-Fcε. Three days after injection, spleens were harvested and cells were stained using Abs to CD45.1 and CD4 and analyzed by flow cytometry. $CD45.1^+CD4^+$ cells were gated, and the levels of CFSE and CTV were examined. (**B**) hFcεRI-dependent presentation of OVA in hFcεRIα-Tg mice injected with OVAp-Fcε. hFcεRIα-Tg mice and non-Tg control mice were adoptively transferred with CTV-labeled $CD45.1^+CD4^+$ OT-II T cells 1 d before they were injected i.v. with OVAp-Fcε at indicated dosages. Three days after injection, spleens were harvested and cells were stained, and $CD45.1^+CD4^+$ $TCRV\alpha2^+$ cells were analyzed by flow cytometry. Data from hFcεRIα-Tg mice are shown in black and data from non-Tg control mice are shown in gray. (**C** and **D**) hFcεRI-independent presentation of OVA. hFcεRIα-Tg mice and non-Tg control mice were treated and analyzed as described in (B), except that they were injected with 10 μg OVA peptide (323–339) (C) or 50 μg OVA protein (D) instead of OVAp-Fcε. (**E** and **F**) Comparison of OVA presentation in hFcεRIα-Tg mice with or without OVA targeting to hFcεRI. (E) Data from Tg mice injected with 0.1 μg OVAp-Fcε were overlaid with data from Tg mice injected with 10 μg OVA peptide. (F) Data from Tg mice injected with 0.05 μg OVAp-Fcε were overlaid with data from Tg mice injected with 50 μg OVA protein. All data shown in (A)–(E) are representative of three independent experiments.

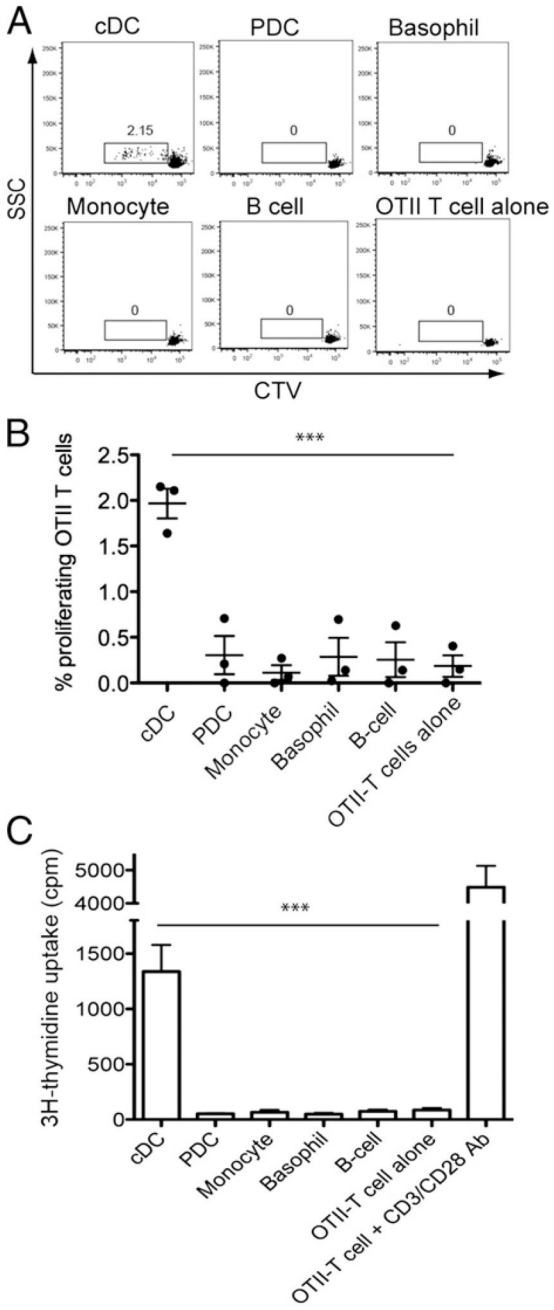

FIGURE 6.

FcεRI-targeted Ags are presented specifically by cDCs in hFcεRIα-Tg mice. (**A** and **B**) hFcεRIα-Tg mice were injected i.v. with 0.2 μg OVAp-Fcε. Twenty-four hours later, spleens were harvested. cDCs ($CD11c^{hi}$), PDCs ($mPDCA1^{+}$), basophils ($Dx5^{+}CD131^{+}$), monocytes ($CD11b^{+}GR1^{med/low}$), and B cells ($CD19^{+}$) were isolated by FACS, mixed with CTV-labeled $CD45.1^{+}$ $CD4^{+}$ OT-II T cells at a 1:5 ratio, and cultured at 37°C. As a negative control, CTV-labeled $CD45.1^{+}$ $CD4^{+}$ OT-II T cells were cultured alone. Three days later, cells were harvested, stained using Abs to CD45.1, CD4, and TCRVα2, and analyzed by flow cytometry. $CD45.1^{+}CD4^{+}TCRV\alpha2^{+}$ cells were gated and the percentage of CTV-

dilution was determined. Shown in (A) are data from one representative experiment. Shown in (B) are data from three independent experiments including mean ± SEM. (**C**) hFcεRIα-Tg mice were injected i.v. with 1 μg OVAp-Fcε. Twelve hours later, spleens were harvested and cells were isolated by FACS as described in (A) and (B), mixed with OT-II $CD4^+$ T cells at a 1:10 ratio, and cultured at 37°C for 4 d. [^{3}H]Thymidine was added for the last 15 h of the culture. As a positive and negative control, OT-II $CD4^+$ T cells were cultured in the presence or absence of anti-CD3/anti-CD28 Ab. Experiments were performed twice as quadruplicates and data show one representative experiment including mean ± SEM. ***$p < 0.005$.

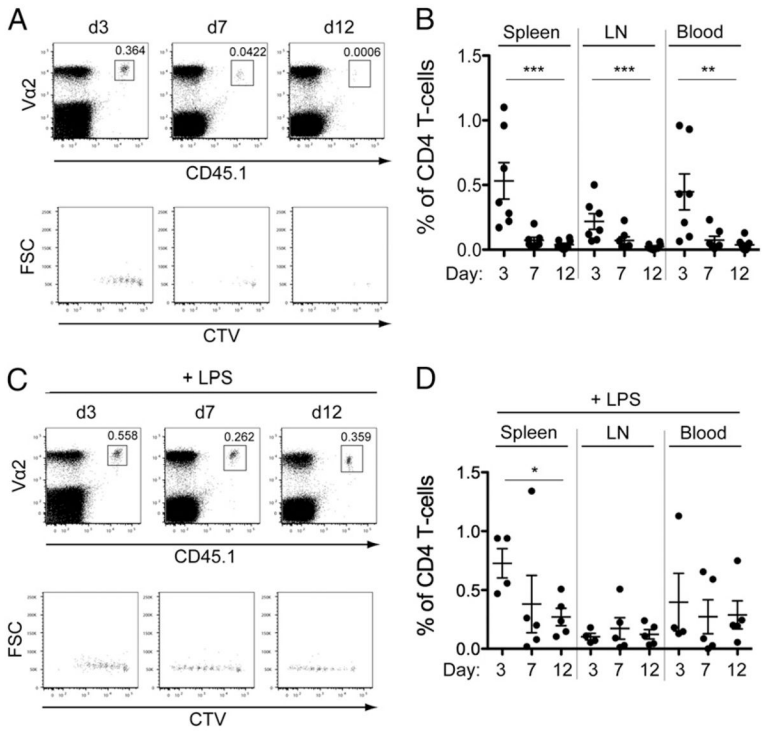

FIGURE 7.

Ag targeting to FcεRI results in Ag-specific $CD4^+$ T cell deletion in hFcεRIα-Tg mice. (**A** and **B**) Rapid deletion of OT-II $CD4^+$ T cells in hFcεRIα-Tg mice injected with OVAp-Fcε. hFcεRIα-Tg mice were adoptively transferred with CTV-labeled $CD45.1^+$ OT-II $CD4^+$ T cells 1 d before they were injected i.v. with 0.2 μg OVAp-Fcε. Three, seven, and twelve days after injection, spleens, inguinal lymph nodes, and blood were harvested. Cells from each tissue were stained and analyzed by flow cytometry for the frequency and extent of CTV dilution of $CD45.1^+$ $TCRV\alpha2^+$ $CD4^+$ cells. Shown in (A) is spleen cell analysis data of one representative experiment. Shown in (B) are spleen, lymph node, and blood cell analysis data with mean ± SEM from four independent experiments analyzing one to three mice per group in each experiment. **(C** and **D)** Persistence of OT-II $CD4^+$ T cells in hFcεRIα-Tg mice injected with OVAp-Fcε and LPS. Mice were treated and analyzed similarly to (A) and (B) with the addition of 3 μg LPS to OVAp-Fcε injection. Data in (D) are from two independent experiments analyzing two or three mice per group in each experiment. $*p < 0.05$, $**p < 0.01$, $***p < 0.005$.

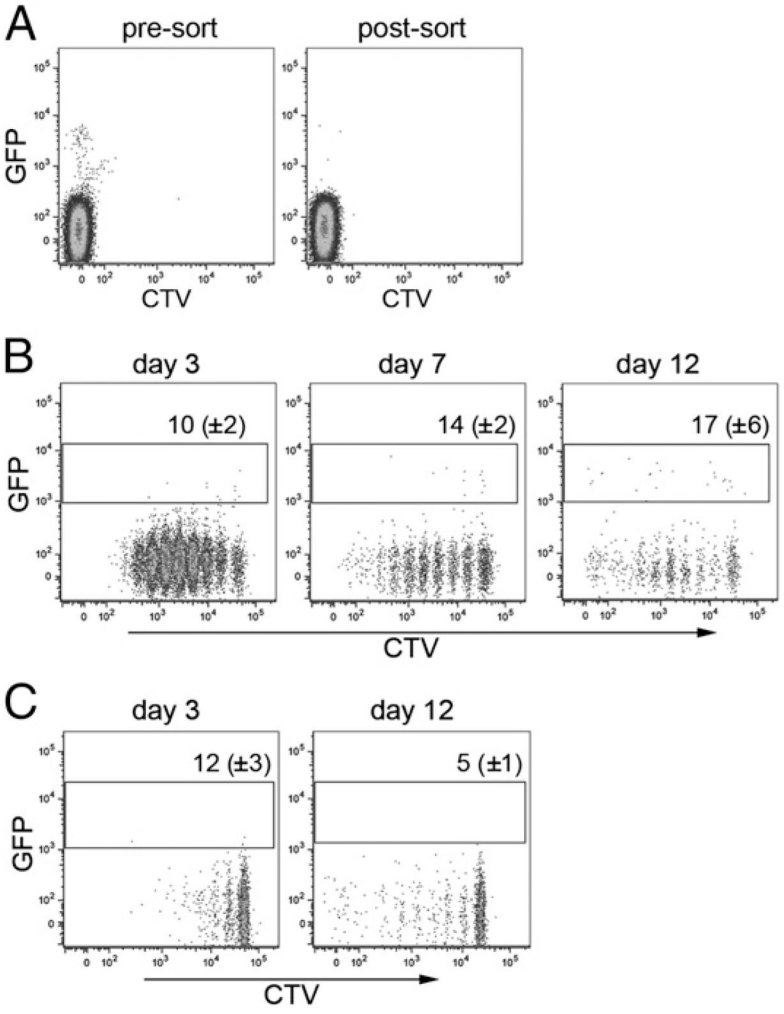

FIGURE 8.

Ag targeting to FcεRI results in induction of few Ag-specific regulatory T cells in hFcεRIα-Tg mice. (**A**) Isolation of nonregulatory OT-II $CD4^+$ T cells by FACS. $CD4^+$ T cells were isolated from $Foxp3^{GFP}$OT-II mice by using anti-CD4 Ab magnetic beads, and GFP^- cells were subsequently isolated by FACS. **(B** and **C)** Induction of few OT-II Treg cells in hFcεRIα-Tg mice injected with OVAp-Fcε. hFcεRIα-Tg mice adoptively transferred with CTV-labeled $Thy1.1^+Foxp3^-$OT-II $CD4^+$ T cells were injected i.v. with 0.2 μg (B) or 0.03 μg (C) of OVAp-Fcε. At indicated days, $CD4^+$ T cells were isolated from whole spleen and analyzed by flow cytometry. GFP^+ cells among OT-II $CD4^+$ T cells ($CD4^+Thy1.1^+TCRV\beta5^+$ cells) were gated as shown in rectangles. Number of these cells is shown as mean ±SEM. Data in (B) represent one experiment using three mice per group. Data in (C) represent two experiments using four mice per group in each experiment.

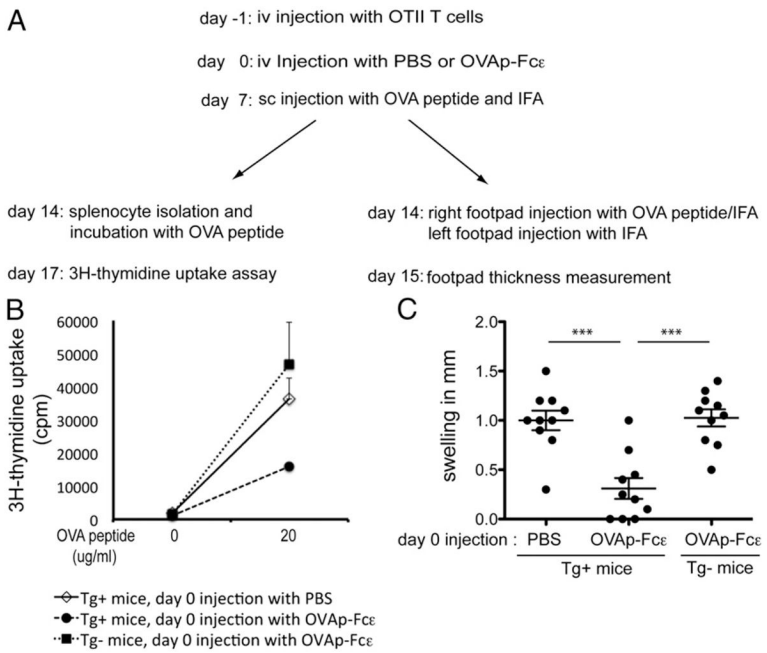

FIGURE 9.

Administration of Ag-Fcε fusion proteins inhibits development of Ag-specific T cell immunity in hFcεRIα-Tg mice. (**A**) Experimental scheme. (**B**) [^{3}H]Thymidine uptake assay. Experiments were performed twice using three mice per group in each experiment. Data show one representative experiment with mean ± SEM. (**C**) DTH assay. Thickness of right footpad subtracted by that of left footpad is indicated as “swelling.” Experiments were performed three times using three to four mice per group in each experiment. Data represent mean ± SEM of measurements made from total 10 mice for each group. ***$p < 0.005$.